J Electroceram (2008) 21:78–84
DOI 10.1007/s10832-007-9080-z

Ferroelectric and magnetoelectric behaviors of multiferroic $BiFeO_3$ and piezoelectric-magnetostrictive composites

J.-M. Liu · F. Gao · G. L. Yuan · Y. Wang · M. Zeng · J. G. Wan

Published online: 23 March 2007

Abstract In this paper we overview our recent work on ferroelectric and magnetoelectric coupling behaviors of multiferroic doped $BiFeO_3$ (BFO) and piezoelectric-magnetostrictive composites. Using rapid liquid sintering method we prepare single-phase BFO ceramics of excellent ferroelectric property. The BFO thin films on *Pt*-coated silicon wafers by pulsed laser deposition show large remnant polarization but serious ferroelectric switching fatigue. A series of piezoelectric-magnetostrictive composite structures in bulk and thin film forms are prepared and giant magnetoelectric coupling effect of them is observed. The experimentally measured results are confirmed by numerical modeling based on piezoelectric and magnetostrictive constitution equations.

Keywords Multiferroics · Magnetoelectric coupling · Piezoelectric · Magnetostrictive

PACS Numbers 75.80.+q · 77.55.+f · 75.70.Ak

1 Introduction

Multiferroics, also called ferroelectromagnets, represent a broad class of materials possessing two or more types of switchable states for memory and transducer applications [1, 2]. In most cases, ferroelectric polarization *P*, magnetization *M* and magnetoelectric (ME) coupling between them are the frequently studied topics. It has been expected that fluctuations in *P* or *M* can be activated upon applying external magnetic field *H* or electric field *E*, respectively. This triggers quite a few proposed novel devices utilizing this additional degree of freedom besides *P* and *M* themselves [3, 4].

In one hand, quite a number of single-phase multiferroic compounds have been studied, focusing on the phase transitions associated with ferroelectric ordering and magnetic ordering as well as their coupling, noting that the ME coupling is usually weak [5, 6]. However, the recently very aggressive experimental findings revealed a reversible polarization upon time-varying magnetic field in $TbMn_2O_5$, [7] and giant polarization and ME coupling effect in strained $BiFeO_3$ thin films, [8] stimulating massive research activities along this line. Although the detected polarization change upon a magnetic field *H* of ~Tesla is only ~nC/cm^2, the well-reproduced polarization reversal induced by the time-varying *H* is impressive. For the strained ultra-thin film BFO, a remnant polarization of ~10 μC/cm^2 at room temperature, comparable to $Pb(Zr,Ti)O_3$, was reported.

On the other hand, the most promising materials in terms of realistic applications reserve for artificially prepared multiferroics in which typically piezoelectric (PE) materials and magnetostrictive (MS) ones are combined to form PE-MS composite multiferroics [9, 10]. Upon different types of combinations, such as 0–3, 1–3 and 2–2 forms, these multiferroics may exhibit giant ME coupling effect via the effective mechanical transfer on the two-phase interface. The recorded ME coefficient so far is up to ~10 V/cm·Oe at the resonance point [11].

Nevertheless, some challenges remain there in terms of realistic applications. For BFO, the intrinsic polarization is

J.-M. Liu (✉) · F. Gao · G. L. Yuan · Y. Wang · M. Zeng · J. G. Wan
Nanjing National Laboratory of Microstructures, Nanjing University,
Nanjing 210093, People's Republic of China
e-mail: liujm@nju.edu.cn

J.-M. Liu · F. Gao · G. L. Yuan · Y. Wang · M. Zeng · J. G. Wan
International Center for Materials Physics, Chinese Academy of Sciences,
Shenyang, People's Republic of China

still very small and the high leakage current which makes the ferroelectric measurement catastrophic is one of the main drawbacks for applications [12]. The reason for high leakage current is the existence of Fe^{2+} ions and high density of oxygen vacancies (OVs) due to preferred evaporation of Bi^{3+} and variable Fe^{2+} and Fe^{3+} during materials sintering. It has been a popular strategy to perform A-site doping of BFO by rare-earth ions in order to enhance the polarization, and to sinter pure BFO perovskite phase in order to reduce the leakage current [13, 14]. At the same time, the inhomogeneous spiral antiferromagnetic (AFM) configuration of rhombohedral BFO can be broken by La-doping at A-site, while a homogeneous AFM configuration in tetragonal structure can be achieved [15].

For the composite multiferroics, the issues to be concerned include size minimization and synthesis of thin film composites of giant ME effect. In this paper, we report our recent works on these issues and several types of composite structures developed in our laboratory. We will first overview the rapid liquid sintering processing of bulk ceramics and pulsed laser deposition of thin films for BFO doped with La. Subsequently, we describe our recent efforts in synthesizing various PE-MS multiferroic composites of giant ME coupling effect.

2 Experimental details and synthesis of composite structures

2.1 Ceramics and thin films of BFO

The standard solid-state reaction sintering of BFO results in loss of Bi^{3+} and a high density of OVs and also formation of impurities other than ABO_3-phase, which are responsible for the large leakage and small saturation polarization. In order to avoid the Bi^{3+}-deficiency and accelerate the kinetics of chemical reaction between constitutions during sintering, a rapid liquid sintering technique has been developed and a detailed description can be found elsewhere [12]. By this sintering method, high quality and singe-phase BFO ceramics can be synthesized, which exhibits a dc-resistivity of 10^9 Ω·cm and a breaking voltage much higher than 150 kV/mm at room temperature.

The same technique was used to synthesize La-doped BFO, where high purity La_2O_5 powders were weighed in stoichiometric proportion $(Bi_{1-x}La_x)FeO_3$ (BLFO) and mixed with Bi_2O_3 and Fe_2O_3 powders for the rapid liquid sintering. The synthesized samples were measured for their crystalline structures using X-ray diffraction and ferroelectric properties using a RT6000 ferroelectric tester under virtual ground conditions. The BLFO thin films of ~250 nm in thickness were deposited on $Pt/TiO_2/SiO_2/(100)Si$ substrates by excimer laser ablating of the ceramic target of the same constitution and their structure and ferroelectric properties were measured subsequently. The pulsed laser beam of 248 nm in wavelength, 30 ns in pulse width and 6 Hz in reprate was employed. The laser fluency was 400 mJ with a spot of density of ~2.0 J/cm^2. The substrate temperature was 500 to 650 °C and the deposition was performed in flowing oxygen ambient of 10 Pa pressure.

2.2 PE-MS multiferroic composites

We have successfully fabricated several PE-MS composite structures in order to obtain giant ME coupling effect. The first two-component composite structure composed of magnetostrictive Terfenol-D ($Tb_{0.27-0.30}Dy_{0.73-0.70}Fe_{1.90-1.95}$) powder mixed with epoxy resin and PZT-502 ($PbZr_{0.52}Ti_{0.48}O_3$) ceramic powder mixed with epoxy resin takes a rectangular plate shape. The two components are connected through the lateral interface coupling, and the applied ac-magnetic field and the generated voltage are

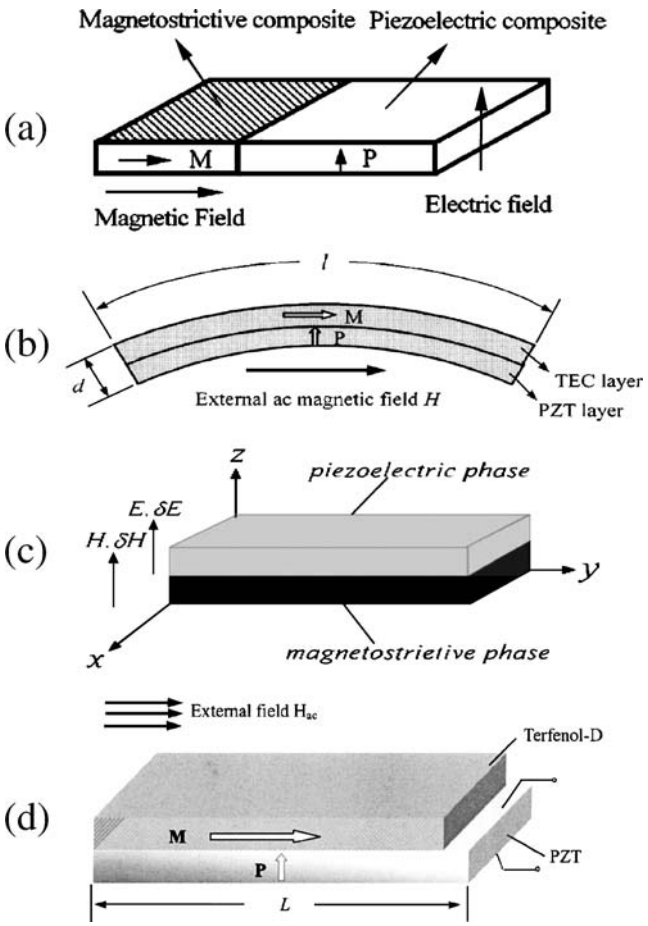

Fig. 1 Schematic drawings of several simple PE-MS composite structures developed in our laboratory. (**a**) Laterally connected two-component structure; (**b**) Bilayered two-component structure with bending mode; (**c**) Bilayered structure and (**d**) Multilayered structure in which the two components are connected in series or parallel form

indicated in Fig. 1(a). The details of the synthesis procedure was reported earlier [11]. Also, the bilayered Terfenol-D/PZT structures were fabricated [16], as shown in Fig. 1(b). The former structure operates at a longitudinal vibrating mode while the latter one operates at a bending vibrating mode, through the interfacial coupling between the two components.

The second two-component bilayered structure as schematically shown in Fig. 1(c) is composed of piezoelectric PZT502 and Ni-ferrite/Co-ferrite powders (NFO/CFO), respectively. This combined structure is operated by the longitudinal vibrating mode, generating the ME coupling effect. The bilayered composite samples of NFO-PZT and CFO-PZT were synthesized from two individual phases and the detailed procedure of synthesis can be found in our previous report [17, 18].

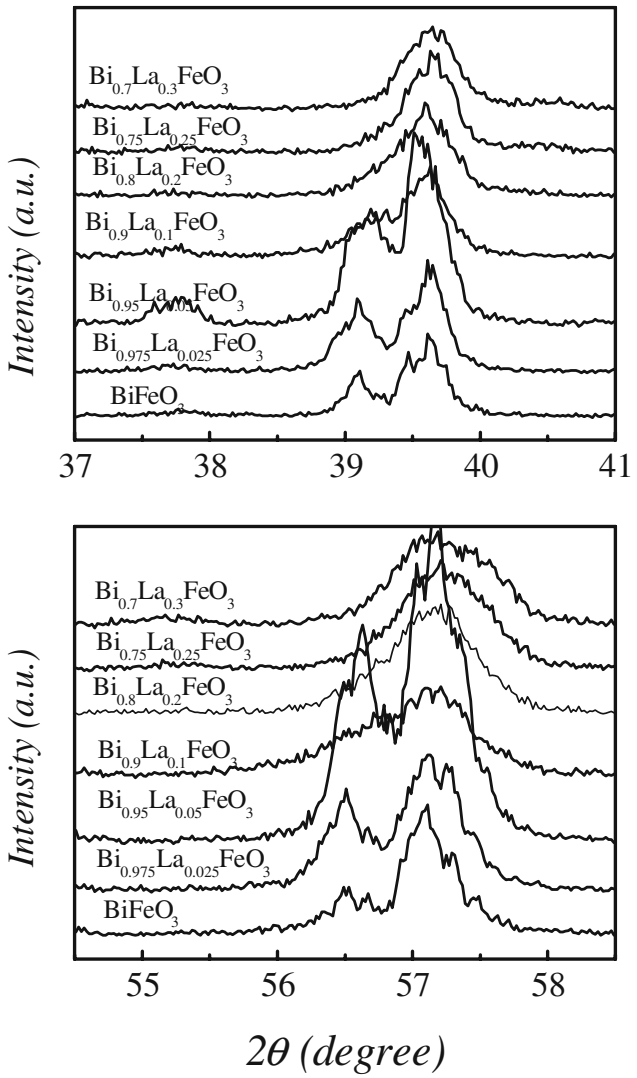

Fig. 2 Parts of the X-ray diffraction spectra of $Bi_{1-x}La_xFeO_3$ ceramics prepared by rapid liquid sintering method (x=0.0 to 0.3)

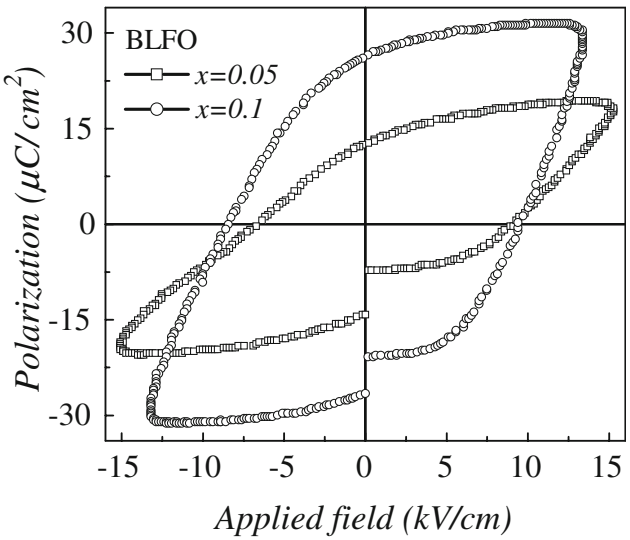

Fig. 3 Measured ferroelectric hysteresis of $Bi_{1-x}La_xFeO_3$ ceramics (x= 0.05 and 0.1), sintered by rapid liquid sintering method

The third structure is in a multi-layered configuration in which the Terfenol-D plates and PZT plates were stacked in a series mode and a parallel mode, respectively, in order to improve the ME coupling spectrum as a function of frequency of the activating ac-field. A schematic drawing of one unit for the series and parallel connections is given in Fig. 1(d). One may refer to our earlier report on the details of fabrication [19].

The last but not the least structure fabricated in our laboratory is the thin film composite of PZT and CFO, where the fine CFO particles are randomly distributed in the matrix of PZT. It exhibits significant ME coupling effect ever demonstrated in thin film composite systems [20]. A numerical calculation by Nan et al [21] predicted that such a composite structure is favored for a significant change of polarization upon a magnetic field.

3 Results and discussion

3.1 Bulk BFO ceramics doped with La

Figure 2 shows the XRD spectra for a series of BLFO samples synthesized at different temperatures by the rapid liquid sintering technique. As well known, BFO has a rhombohedral structure which shows split reflections at 2θ= 39.5° and 57.2°. With increased La-doping up to x=0.3, the splitting of the two reflections disappears at $x \geq 0.1$ because the structure changes from rhombohedral to tetragonal. It was reported earlier that the tetragonal BLFO is of spatially homogeneous FM ordering, which benefits to the ME coupling [15].

The sintered BLFO ceramics show excellent ferroelectric property with a resistivity as high as 10^9 Ω·cm, and a breaking field much larger than 150 kV/cm. The ferroelectric hysteresis is shown in Fig. 3 at x=0.05 and 0.1. Although the hysteresis is not yet well-saturated, the measured remnant polarization is as big as 25 μC/cm^2 as x=0.1. This value is already much bigger than that for pure BFO, 8~10 μC/cm^2 in the present case. Further increasing of x from x=0.1 will result again in slight decreasing of the remnant polarization, while the structure becomes completely tetragonal.

3.2 Thin film BLFO

We prepare BFO and BLFO (x=0.2) thin films respectively at a substrate temperature T_s=550 °C and the films show perfect tetragonal structure, same as the ceramic samples.

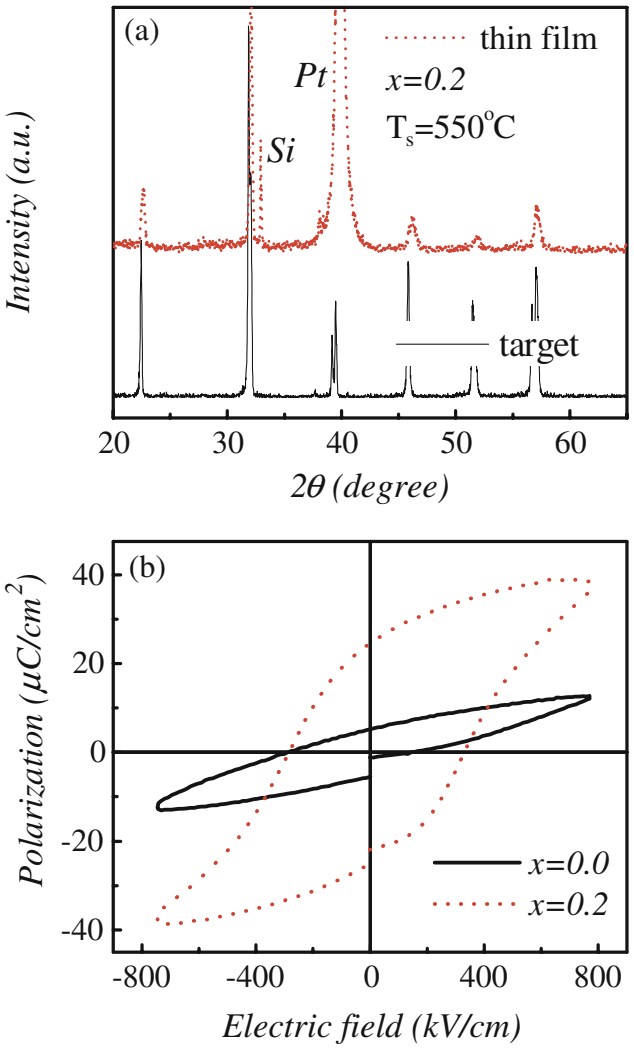

Fig. 4 (**a**) X-ray diffraction spectra of $Bi_{1-x}La_xFeO_3$ ceramic target and thin film deposited at 550 °C on Pt-coated (100) Si wafers, and (**b**) ferroelectric hysteresis loops of the thin films (x=0.0 and 0.2)

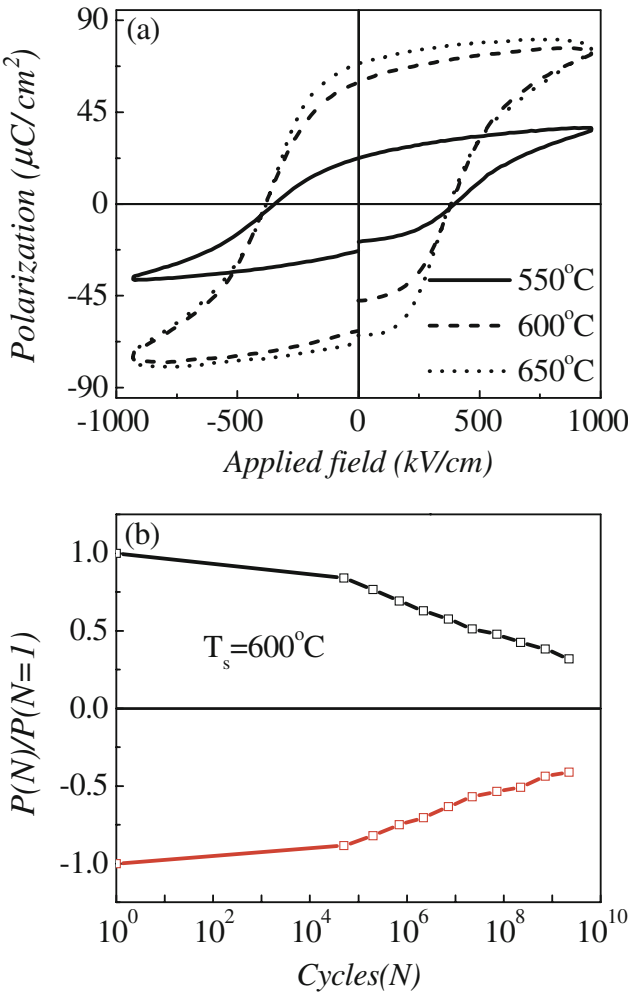

Fig. 5 (**a**) Ferroelectric hysteresis loops for the $Bi_{1-x}La_xFeO_3$ (x=0.2) thin films deposited at 550, 600 and 650 °C, respectively. (**b**) Ferroelectric switching fatigue for the thin film (x=0.2) deposited at 600 °C

As an example, Fig. 4(a) presents the XRD spectra of the BLFO target and thin films as prepared. The thin film shows the same tetragonal structure as the target. Figure 4(b) shows the measured ferroelectric hysteresis for the prepared BFO and BLFO thin films. Similar to the ceramic samples, the BLFO shows excellent ferroelectric property with the saturated and remnant polarizations of 40 and 25 μC/cm^2, respectively. These values are comparable to those for PZT and meet the requirement for potential applications.

The deposition temperature for the thin films has significant effect on the ferroelectric property. In Fig. 5(a) are plotted the measured loops of three BLFO (x=0.2) thin films deposited at 550, 600 and 650 °C, respectively. It is surprising to observe that the 600 and 650 °C prepared samples exhibit much better ferroelectric property than the 550 °C thin film. The saturated and remnant polarizations reach up to 75 and 60 μC/cm^2, respectively. These values are among the ever highest reported so far. And it is demonstrated that La-doping does improve the ferroelectric

property of BFO. The ferroelectric fatigue behavior of BLFO is investigated too, and the room temperature data are plotted in Fig. 5(b). Although the fatigue endurance of BLFO thin films on STO substrates were measured at a pulse frequency of 100 kHz, indicating no fatigue up to cycles of 10^{10}, serious fatigue effect is observed for the present samples. The reason is that the present data was obtained at the frequency of 50 kHz where an effective switching is achieved in one hand, and on the other hand, the present samples were deposited on Pt-coated Si substrates.

3.3 ME coupling in bulk PE-MS composite structures

We focus on the ME coupling effect as obtained in different types of PE-MS composite structures. In Fig. 6(a) is shown the measured ME coupling coefficient α for the structure shown in Fig. 1(a) as a function of frequency f of the *ac*-activating magnetic field H_{ac} plus to three bias field H_{bias},

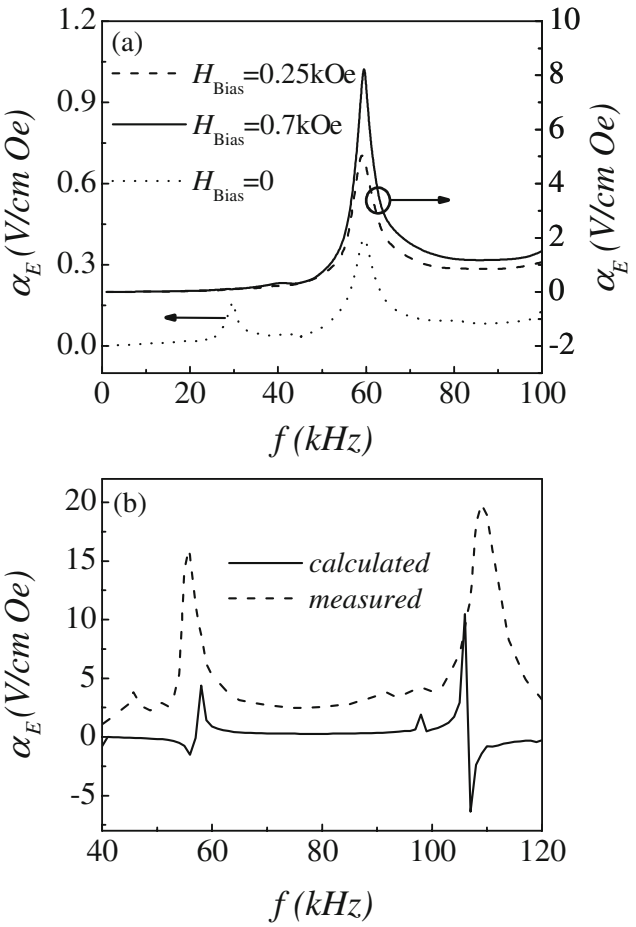

Fig. 6 (**a**) Measured ME coupling coefficient as a function of frequency of activating ac-magnetic field under three different dc-bias magnetic fields, for the two-component structure shown in Fig. 1(a). (**b**) Measured and calculated ME coupling coefficient as a function of frequency under an optimized dc-magnetic field

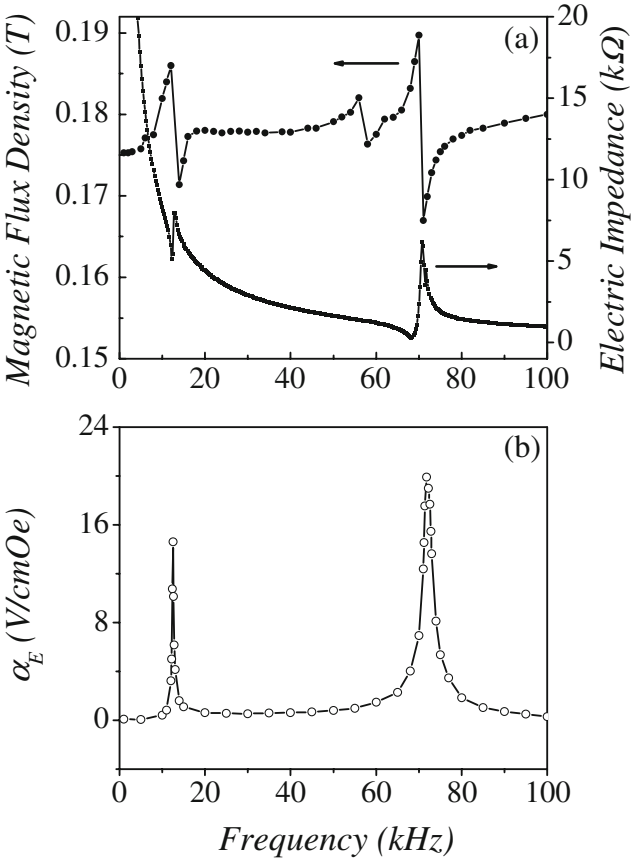

Fig. 7 (**a**) Measured magnetic flux density and electrical impedance and (**b**) ME coupling coefficient as a function of frequency of activating ac-magnetic field for the bilayered bending structure shown in Fig. 1(b)

where the MS component has a size of 6.8 mm (length)× 6.2 mm×0.7 mm and the PE component has a size of 8.0 mm (length)×6.2 mm×0.7 mm [11, 22]. At the resonant frequency of 60 kHz with H_{bias}=0.7 kOe, the peaked value of α is as high as 8.0 V/cm·Oe, one of the highest values ever.

We proposed a finite-element numerical algorithm based on the piezoelectric and magnetostrictive constitution equations to calculate the coupling coefficient as a function frequency [23]. The constitution equations for the MS component can be written as:

$$\begin{aligned} \sigma &= C^H \varepsilon - d\,H \\ B &= d^T\,\varepsilon + \mu^\varepsilon\,H \end{aligned} \tag{1}$$

where σ and ε denote the stress and strain in MS, B and H are the magnetic flux and magnetic field strength, while C^H, d and μ^ε are the elastic stiffness constants at a fixed H, magnetostrictive coupling coefficients and magnetic permeability at constant strain, respectively. The constitutive relation for PE component can be written as:

$$\begin{aligned} \sigma &= C^E\varepsilon - e\,E \\ D &= e^T\varepsilon + \lambda^\varepsilon\,E \end{aligned} \tag{2}$$

where σ and ε denote the stress and strain in PE, D and E are the electric displacement and electric field, C^E, e and λ^ε are the elastic stiffness constants at a fixed E, piezoelectric coefficients and dielectric constants at constant strain, respectively.

The calculated spectrum and the experimentally measured one for an optimized structure are presented in Fig. 6(b) [23]. A good quantitative consistency between them is shown.

For the composite structure shown in Fig. 1(b), where the bilayer is stacked and bonded with the rectangle Terfenol-D/Epoxy composite (TEC) and PZT-5 piece with epoxy binder, we observed two types of vibrating modes for the ME coupling. Both TEC and PZT layers have the same sizes of 17.4 mm (length)×4.5 mm (width)×0.72 mm

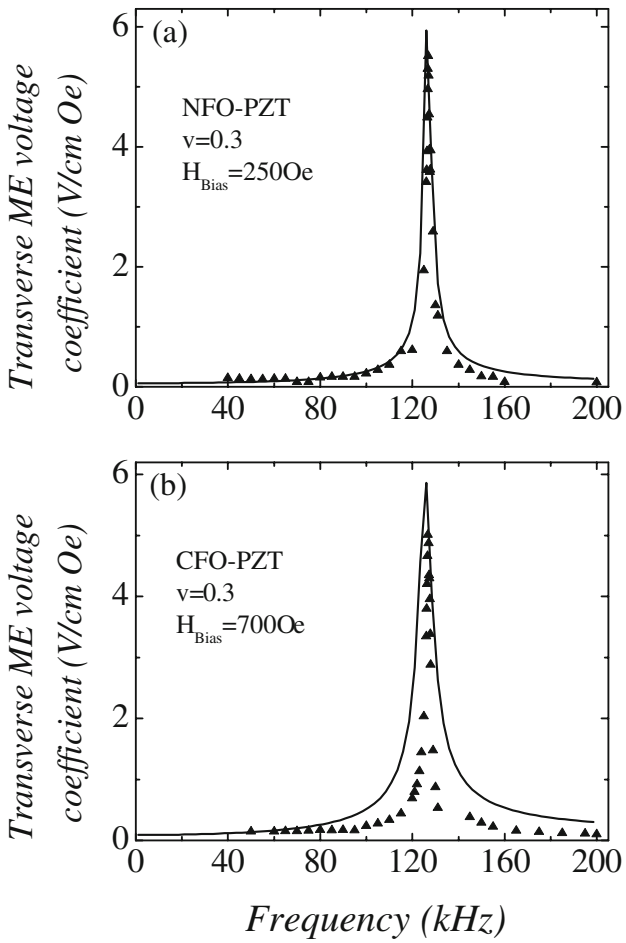

Fig. 8 Comparison of the calculated ME voltage coefficient with respect to the frequency response with the experimental data. The *solid lines* are the calculated results of the frequency dependence of the transverse ME voltage coefficient for (**a**) NFO-PZT and (**b**) CFO-PZT bilayers. Estimates are for the thickness and width much smaller than the length. The resonance character is noticeable. Parameters used for the estimates were given in [17]. The *triangles* are data points for NFO-PZT and CFO-PZT bilayers with 4-mm width and 2-mm thickness. The *lines* are guides to the eye

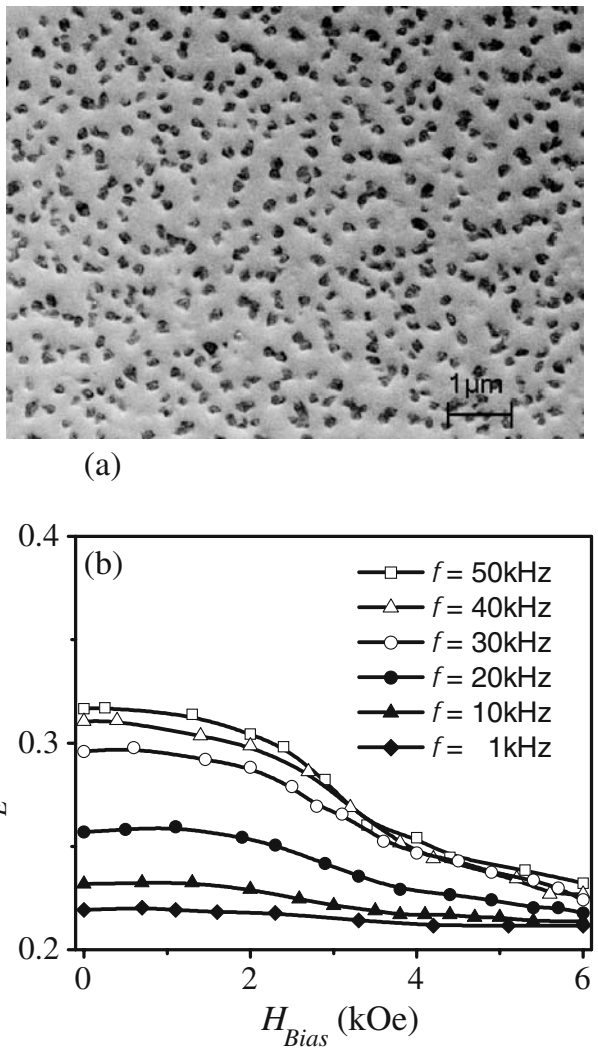

Fig. 9 (**a**) Scanning electron microscopy image of the CFO-PZT thin film, where black particles are CFO and the matrix is PZT. (**b**) Measured ME coupling coefficient as a function of dc-biased magnetic field with different frequencies of activating ac-magnetic field

(thickness). The magnetic flux density and electrical impedance as well as the coupling coefficient as a function of frequency is shown in Fig. 7(a) and (b), respectively. The higher frequency peak of α corresponds to the longitudinal vibrating mode while the lower frequency peak is for the first-order bending mode. The giant ME coupling effect is demonstrated [16].

The rectangular bilayer composites of magnetostrictive ferrites and PZT were fabricated, as shown in Fig. 1(c). The giant ME effects were observed at the frequency of 126.9 kHz for nickel ferrite (NFO)/$Pb(Zr_{0.52}Ti_{0.48})O_3$ (PZT) and cobalt ferrite (CFO)/PZT composites. The measured peak values of ME voltage coefficients were 5.5 and 5.0 V/cm·Oe for the two samples. This frequency-dispersive ME effect is explained by solving the equation of motion in the 1-Dimension homogeneous medium. The

numerically simulated results show excellent consistence with the experimental data, as shown in Fig. 8(a) and (b), where v is the volume fraction of PZT [18].

One of the major drawbacks for the composite structure is that the ME coupling aside from the resonance point is quite low, while the resonance peak remains very sharp. This enables realistic applications to be difficult since the frequency shift is often inevitable in practice. To overcome this drawback, we prepared a set of Terfenol-D/PZT bilayers with slightly different lengths and packaged them together in series and parallel forms, respectively, and then measured the ME coupling coefficient as a function of frequency of activating magnetic field. The measured giant ME effect of the series packaged composite structure showed a much broader frequency response to external field than a single bilayered structure, and the ME effect aside the resonance ranges was enhanced significantly too. A qualitative analysis based on the equivalent circuit concept was presented to explain these novel effects [19].

3.4 ME coupling in thin film PE-MS composite

From the point of view of integrated applications of ME composites, thin film composites with giant ME effect are required. We prepared CFO-PZT composite thin films using a sol–gel process and spin-coating technique [20]. In the microstructures, the well crystallized CFO and PZT phases are separated and the magnetic CFO particles distribute randomly on the matrix of PZT phase, as shown in Fig. 9(a), although the distribution of CFO particles are not in an ordered form, as predicted by Nan et al in terms of optimized ME coupling [21]. Vibrating sample magnetometer and ferroelectric tester were used to characterize the magnetic and ferroelectric properties. The prepared films exhibit both good magnetic and ferroelectric properties, as well as a unique ME effect. The measured ME coupling coefficient as a function of the dc-biased magnetic field at different frequencies for the ac-magnetic field is presented in Fig. 9(b). A high initial coefficient for the film is observed. The ME effect of the film strongly depends on the magnetic bias and magnetic field frequency.

4 Conclusion

In conclusion, we have performed detailed investigations on preparations of single-phase $BiFeO_3$ ceramics doped with La and various piezoelectric-magnetostrictive composite structures, including two-component connected, bilayered and thin film structures, and characterized their ferroelectric, magnetic and magnetoelectric coupling behaviors. The piezoelectric component is $Pb(Zr_{0.52}Ti_{0.48})O_3$ and the magnetostrictive component is Terfenol-D, CoFe2O4 and NiFe2O4 etc. By La-doping, $BiFeO_3$ both in bulk and thin film forms exhibits promising ferroelectric property, while the magnetoelectric coupling is waiting for further enhancement. On the other hand, the several composite structures fabricated in our laboratory are very promising for potential applications because all of them exhibit giant ME coupling effect.

Acknowledgement This work was supported by the National Nature Science Foundation of China (10474039, 50372020 and 10021001), the National Key Project for Basic Researches of China (2002CB613303), and LSSMS of Nanjing University.

References

1. G.A. Smolenski, I.E. Chupis, Sov. Phys., Usp. **25**, 475 (1982)
2. H. Schmid, Ferroelectrics **162**, 317 (1994)
3. T.H. O'Dell, Electron. Power **11**, 266 (1965)
4. L.P.M. Bracke, R.G. van Vliet, Int. J. Electron **51**, 255 (1981)
5. Y.N. Venevtsev, V.V. Gagulin, Ferroelectrics **162**, 23 (1994)
6. M.I. Bichurin, Ferroelectrics **204**, xvii (1997)
7. N.Hur, S. Park, P.A. Sharma, J.S. Ahn, S. Guha, S.W. Cheong, Nature **429**, 392 (2004)
8. J. Wang, J.B. Neaton, H. Zheng, V. Nagarajan, S.B. Ogale, B. Liu, D. Viehland, V. Vaithyanathan, D.G. Schlom, U.V. Waghmare, N. A. Spaldin, K.M. Rabe, M. Wuttig, R. Ramesh, Science **299**, 1719 (2003)
9. C.-W. Nan, Phys. Rev. B **50**, 6082 (1994)
10. C.-W. Nan, M. Li, Appl. Phys. Lett. **78**, 2527 (2001)
11. J.G. Wan, J.-M. Liu, H.L. W. Chan, C.L. Choy, G.H. Wang, C.W. Nan, J. Appl. Phys. **93**, 9916 (2003)
12. Y.P. Wang, L. Zhou, M.F. Zhang, X.Y. Chen, J.-M. Liu, Z.G. Liu, Appl. Phys. Lett. **84**, 1731 (2004)
13. T. Kanai, S.I. Ohkoshi, K. Hashimoto, J. Phys. Chem. Solids **64**, 391 (2003)
14. M.M. Kumar, V.R. Palkar, K. Srinivas, S.V. Suryanarayana, Appl. Phys. Lett. **76**, 2764 (2000)
15. A.V. ZalesskiĬ, A.A. Frolov, T.A. Khimih, A.A. Bush, Phys. Solid State **45**, 141 (2003)
16. J.G. Wan, Z.Y. Li, Y. Wang, M. Zeng, G.H. Wang, J.-M. Liu, Appl. Phys. Lett. **86**, 202504 (2005)
17. M. Zeng, J.G. Wan, Y. Wang, H. Yu, J.-M. Liu, X.P. Jiang, C.W. Nan, J. Appl. Phys. **95**, 8069 (2004)
18. Y. Wang, H. Yu, M. Zeng, J.G. Wang, M.F. Zhang, J.-M. Liu, C. W. Nan, Appl. Phys. A S003390042983-5 (2004)
19. H. Yu, M. Zeng, Y. Wang, J.G. Wan, J.-M. Liu, Appl. Phys. Lett. **86**, 032508 (2005)
20. J.G. Wan, X.W. Wang, Y.J. Wu, M. Zeng, Y. Wang, H. Jiang, W. Q. Zhou, G.H. Wang, J.-M. Liu, Appl. Phys. Lett. **86**, 122501 (2005)
21. C.W. Nan, G. Liu, Y.H. Lin, H. Chen, Phys. Rev. Lett. **94**, 197203 (2005)
22. J.G. Wan, S.W. Or, J.-M. Liu, H.L.W. Chan, G.H. Wang, C.W. Nan, IEEE Trans. Magn. **40**, 3042 (2004)
23. Y. X. Liu, J. G. Wan, J.-M. Liu, C. W. Nan, J. Appl. Phys. **94**, 5111, 5118 (2003)